Identification of the form of self-excited aerodynamic force of a bridge deck based on machine learning

Zeyu Zhang [1,2], Shujin Laima[1,2*], Hui Li [1,2]

[1] *Key Lab of Smart Prevention and Mitigation of Civil Engineering Disasters of the Ministry of Industry and Information Technology, Harbin Institute of Technology, Harbin 150090, China, laimashujin@hit.edu.cn*
[2] *Key Lab of Structures Dynamic Behavior and Control of the Ministry of Education, Harbin Institute of Technology, Harbin 150090, China*

SUMMART

Flutter and VIV are two typical aerodynamic self-excited vibration phenomena. Over the years, most of the modeling of the aerodynamic equations of flutter and VIV is based on experience[1]. These methods rely too much on prior knowledge and are less universal. This paper proposes an intelligent approach based on machine learning techniques to explore the explicit form of the self-excited aerodynamic equations implicit in the data. This method does not need to assume the form of the aerodynamic equation in advance, and then use the data to fit the coefficients, but automatically explores the explicit form of the equation. Compared with the traditional method, this method has a high degree of intelligence, strong versatility, and has significant advantages. The result is more reasonable and credible. In this paper, taking the bending-torsion coupling flutter with limit cycle characteristics as an example, the identification of aerodynamic equations based on intelligent methods is analyzed.
Keywords: self-excited vibration, machine learning, equation identification.

1. Identification of Limit Cycle Flutter Aerodynamic Equations

1.1. Limit cycle flutter experiment

Wind tunnel experiment is an important means to study problems in the field of wind engineering[2]. In this study, a section model spring suspension system was used to perform limit cycle flutter experiments. The wind tunnel is a closed return wind one (SMCCWT-1), The overall characteristics of the wind farm are well; The model has an aspect ratio of 1:10, with the width of 300mm. The leading-edge angle of the section model is 165°and 180°. The structural characteristics of the section model are shown in Table 1 below.

Table 1. Section Model Structural Properties

Angle	$m(kg)$	$I(kg \cdot m^2)$	$f_h(Hz)$	$f_\alpha(Hz)$
165°	1.768	0.009	2.96	4.58
180°	1.779	0.107	2.95	4.59

1.2. Preprocessing of the experimental data for the algorithm

The leading-edge plate of the section model has an obtuse angle structure, with the vibration of bending and torsion mode. Meanwhile, the torsional mode is dominant. Figure 1 below is a set of limit cycle flutter response comparisons between vertical displacement and torsional angle. In order to reveal the aerodynamic equation behind the data as truly and accurately as possible, the influence of the vertical mode is taken into account in the aerodynamic equation. At the same time, since the torsional amplitude is much larger than the vertical displacement amplitude, and the amplitude is often the most concerned issue in practical engineering, the theoretical analysis of the torsional aerodynamic equation is mainly carried out. The two-degree-of-freedom flutter aerodynamic equation can be expressed as：

$$m(\ddot{h}+2\xi_{s.h}\omega_{s,h}\dot{h}+\omega_{s,h}^{2}h)=F_{se} \tag{1}$$

$$I(\ddot{\alpha}+2\xi_{s,\alpha}\omega_{s,\alpha}\dot{\alpha}+\omega_{s,\alpha}^{2}\alpha)=M_{se} \tag{2}$$

$\xi_{s,h}$ 、 $\xi_{s,\alpha}$ 、 $\omega_{s,h}$ 、 $\omega_{s,\alpha}$ are the nonlinear aerodynamic damping and angular frequency caused by the nonlinear factor of the structure itself such as spring stiffness and friction as well as non-wind-induced aerodynamic effects caused by the relative motion between the model and the air under the condition of still wind.

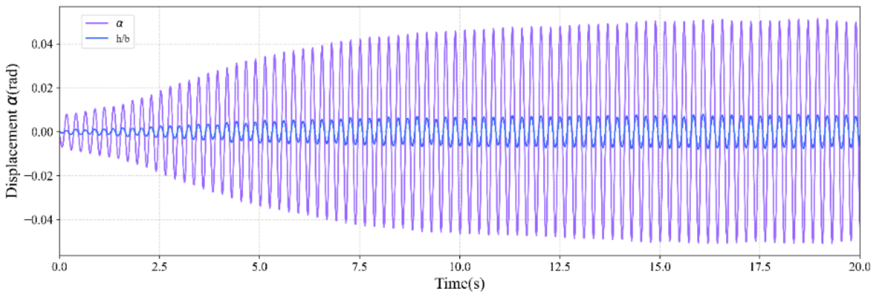

Figure 1. Comparison of vertical displacement amplitude and torsion angle amplitude of limit cycle flutter(180°,U=7.55m/s)

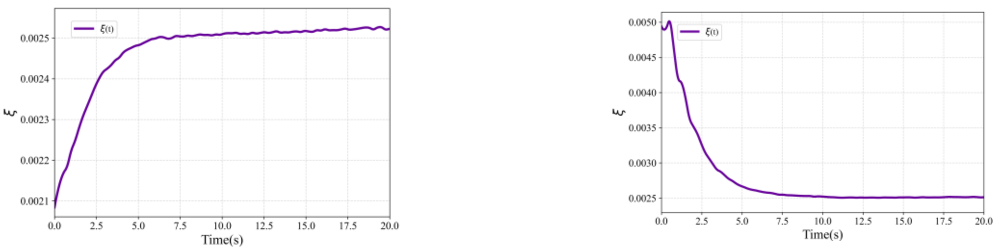

a) small amplitude - steady state   b) large amplitude - steady state

Figure 2. Time history of structural nonlinear damping ratio (180°,U=7.938m/s)

1.3. Recognition results and exploration of the aerodynamic equations

This study borrows and uses a machine learning-based sparse identification algorithm for nonlinear dynamical systems (SINDY)，that is, sequential hard-threshold ridge regression for (STRidge) for sparse identification of aerodynamic equations[3]. The objective function can be expressed as (3). Each meaning of them are shown in(4)-(6); The aerodynamic force with strong nonlinear coupling that coexists with torsion and vertical displacement in a spectacular item is not considered in the candidate dictionary， meanwhile the number of the two modes can be up to six times. It should be noted that a zero-norm regularization term with sparsity is

$$\begin{cases}\xi_M = argmin\left\|M_{se} - \Theta_M \xi_M\right\|_2^2 + \eta\left\|\xi_M\right\|_0 \\ \xi_F = argmin\left\|F_{se} - \Theta_F \xi_F\right\|_2^2 + \eta\left\|\xi_F\right\|_0\end{cases} \tag{3}$$

$$M_{se} = \Theta_M(\alpha,\dot{\alpha},h,\dot{h})\xi_M \text{，} \quad F_{se} = \Theta_F(\alpha,\dot{\alpha},h,\dot{h})\xi_F \tag{4}$$

$$\begin{cases}\Theta_M(\alpha,\dot{\alpha},h,\dot{h}) = [1,\alpha,\dot{\alpha},\cdots,\alpha^6\dot{\alpha}^6,h,\dot{h},\cdots,h^6\dot{h}^6]_{n\times 98} \\ \Theta_F(\alpha,\dot{\alpha},h,\dot{h}) = [1,\alpha,\dot{\alpha},\cdots,\alpha^6\dot{\alpha}^6,h,\dot{h},\cdots,h^6\dot{h}^6]_{n\times 98}\end{cases} \tag{5}$$

$$\begin{cases}\alpha = (\alpha(t_1),\alpha(t_2)\cdots\alpha(t_m))_{m\times 1}^T, \dot{\alpha} = (\dot{\alpha}(t_1),\dot{\alpha}(t_2)\cdots\dot{\alpha}(t_m))_{m\times 1}^T \\ h = (h(t_1),h(t_2)\cdots h(t_m))_{m\times 1}^T, \dot{h} = (\dot{h}(t_1),\dot{h}(t_2)\cdots\dot{h}(t_m))_{m\times 1}^T\end{cases} \tag{6}$$

added to the objective function (3)， The solution to the problem with zero norm is an N-P hard problem, so the STRidge algorithm is used to achieve an equivalent replacement for zero norm optimization； It is worth noting that in the process of algorithm implementation, in order to better achieve sparsity and interpretability, it is necessary to normalize the total aerodynamic data and each item in the dictionary， that is (7)-(8). The aerodynamic term of the equation after

$$M_{se} \to \frac{M_{se}}{\left\|M_{se}\right\|_2}, \theta_M \to \frac{\theta_M}{\left\|\theta_M\right\|_2}, \hat{\xi}_M = \xi_M \frac{\left\|\theta_M\right\|_2}{\left\|M_{se}\right\|_2} \tag{7}$$

$$F_{se} \to \frac{F_{se}}{\left\|F_{se}\right\|_2}, \theta_F \to \frac{\theta_F}{\left\|\theta_F\right\|_2}, \hat{\xi}_F = \xi_F \frac{\left\|\theta_F\right\|_2}{\left\|F_{se}\right\|_2} \tag{8}$$

dimensionless processing can directly reflect the proportion of the aerodynamic term it accounts for. The smaller the coefficient is, the smaller its proportion is. In this way, the sparsity of the sparse results can be further improved-A really little threshold can be set again in the equation identification results to filter items with very small coefficients after normalization. These irregular items with extremely small coefficients can be considered to be caused by the influence of the error brought by the experiment on the algorithm.

After multiple sampling and algorithm verification, it was found that the terms of the torsional aerodynamic equation can be divided into three categories, that is, the aerodynamic stiffness term that affects the conversion between kinetic energy and potential energy in mechanical energy, the aerodynamic damping term that affects the energy transfer between the flow field and the structure, and the pure-force term that does not bear the effects of the above two but only makes the response history fitting more accurate. The aerodynamic terms identified at different angles and wind speeds are stable, and only the coefficients change, indicating that the identification algorithm can accurately reveal the explicit form of the aerodynamic equation. The aerodynamic equation is expressed as the following (9).

$$\begin{aligned} M_{se} = & \underbrace{\varepsilon_{10}\alpha + \varepsilon_{30}\alpha^3 + \varepsilon_{12}\alpha\dot{\alpha}^2 + \tau_{10}h + \varepsilon_{14}\alpha\dot{\alpha}^4}_{Aerodynamic\ stiffness} \\ & + \underbrace{\varepsilon_{01}\dot{\alpha} + \varepsilon_{03}\dot{\alpha}^3 + \varepsilon_{05}\dot{\alpha}^5 + \tau_{01}\dot{h} + \varepsilon_{21}\alpha^2\dot{\alpha} + \varepsilon_{23}\alpha^2\dot{\alpha}^3}_{Aerodynamic\ damping} \\ & + \underbrace{\varepsilon_{20}\alpha^2 + \varepsilon_{02}\dot{\alpha}^2 + \varepsilon_{04}\dot{\alpha}^4}_{pure\ force} \end{aligned} \quad (9)$$

Since the vertical motion is drag motion, the influence of nonlinearity is very small, so although the aerodynamic term about the vertical mode has been increased to the sixth order in the candidate library, only the linear term is identified, that is, the vertical mode linear flutter derivatives. Using the 4-4 Rungr-Kutta method with adaptive step size to predict the response of the identified equation and compare it with the curve obtained from the real experiment, as shown in Figure 3 below. It can be seen that the aerodynamic equation response curve identified

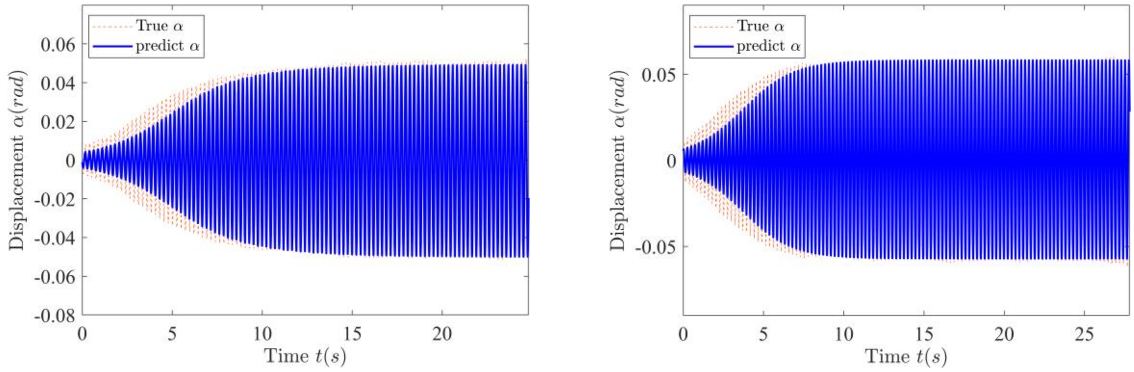

U=7.55m/s U=7.74m/s

Figure 3. Comparison results of torsional curves of flutter experimental and learned equation

by this method fits well with the experiment, indicating the rationality of the results.

Regarding the vertical aerodynamic equation, due to the large proportion of the torsional mode, it contains more complex torsion-related high-order nonlinear terms， and no apparent nonlinear laws are found like torsion aerodynamic equations， this research will be carried out in future work. In each case, the equations contain the linear aerodynamic derivative terms of the two modes， reflecting the rationality of the identified vertical aerodynamic equation.

References:

[1] G. Gao, L. Zhu, J. Li, W. Han, and B. Yao, "A novel two-degree-of-freedom model of nonlinear self-excited force for coupled flutter instability of bridge decks," *Journal of Sound and Vibration*, vol. 480, p. 115406, 2020.

[2] G. Gao, L. Zhu, J. Li, and W. Han, "Application of a new empirical model of nonlinear self-excited force to torsional vortex-induced vibration and nonlinear flutter of bluff bridge sections," *Journal of Wind Engineering and Industrial Aerodynamics*, vol. 205, p. 104313, 2020-1-1 2020.

[3] S. L. Brunton, J. L. Proctor and J. N. Kutz, "Discovering governing equations from data by sparse identification of nonlinear dynamical systems," *Proceedings of the national academy of sciences*, vol. 113, pp. 3932-3937, 2016.